National Conference with International Participation
ENGINEERING MECHANICS 2006
Svratka, Czech Republic, May 15 – 18, 2006
paper no. **294**

STRESS DISTRIBUTION IN HUMAN ARTERY BASED ON SEVERAL TYPES OF SEDF

L. Horný*, T. Adámek†

Summary: *Two material models of an arterial wall based on hyperelastic approach are compared within a solution of a boundary value problem for thick–walled tube. Thick–walled tube, which is the computational model used here, was loaded by internal pressure p = 16 kPa and axial pre–stretches* λ_z *= 1.15, 1.3, 1.45. An influence of residual strains was included. It is shown that purely phenomenological model revealed circumferential Cauchy stress distribution in the range of supposed physiological values. Structural model based on a fiber-reinforcement is significantly more compliant than phenomenological one. Moreover, the residual strains are necessary in the structural model to obtain physiological values of circumferential stress. An influence of an helix angle, which is a structural parameter, on the stress distribution was determined.*

1. Introduction

Most of models describe arterial mechanics using a framework of hyperelastic material. This models are based on assumption that artery is hyperelastic, e.i. on existence of an elastic potential or a *strain energy density function* (SEDF). If any energy density function describes any deformation we can obtain components of a stress tensor as products of differentiation of the SEDF with respect to components of a strain tensor. This approach is suitable to overcome difficulties which are related to description of highly nonlinear mechanical behavior of the arterial tissue.

The aim of this study is to compare two models of the constitutive law of the artery based on hyperelastic approach. The framework of cylindrical thick-walled tube was used in. Geometrical data were obtained from sample of a human abdominal aorta, harvested above a bifurcation close to renal arteries, which were used in our residual strain analysis in 2002. The sample of male abdominal aorta were obtained form cadaver and measurement of an opening angle was done 10 hours after death. A donor was 31 age old man. The measurement was done in Department of Forensic Medicine of University Hospital Na Královských Vinohradech in accordance with laws of the Czech Republic.

* Ing. Lukáš Horný, Department of Mechanics, Faculty of Mechanical Engineering Czech Technical University in Prague, Technická 4, 166 07, Prague, Czech Republic. Tel. +420 224 352 690, fax +420 224 310 292, horny@mbox.fsid.cvut.cz.
† MUDr. MVDr. Tomáš Adámek, Institute of Forensic Medicine, University Hospital Na Královských Vinohradech, Šrobárova 50, 100 34, Prague, Czech Republic. Tel. +420 267 163 571, fax. +420 267 162 505, adamek@fnkv.cz

2. Methods

First model (fully-phenomenological approach) As was shown in many papers the hyperelastic modeling of a mechanical behavior is based on the assumption of the strain energy density function **Ψ** existence. The strain energy density function must satisfy a condition that the material time derivate of **Ψ** is equal the stress power. This condition leads to an equation which means constitutive law for the hyperelastic material. In our case of phenomenological model which does not include the internal structure of the artery we will obtain, see e.g. Hayashi (1996), Holzapfel (1998), Holzapfel (2000),

$$\mathbf{S} = -p\mathbf{C}^{-1} + 2\frac{\partial \boldsymbol{\Psi}(\mathbf{C})}{\partial \mathbf{C}}. \tag{1}$$

This relation is the most general anisotropic stress–strain relation describing incompressible hyperelastic material. **S** is second Piola–Kirchhoff stress tensor defined in a reference configuration, p is the undetermined Lagragian multiplier and **C** is right Cauchy–Green strain tensor. The arterial wall incompressibility is commonly used presumption, see e.g. discussion in Holzapfel (2000). The thick-walled tube model operates with a cylindrical coordinate system with the principal directions $\mathbf{e_t}$ (circumferential), $\mathbf{e_z}$ (axial), $\mathbf{e_r}$ (radial). Here the incompressibility condition leads to

$$\lambda_t \lambda_z \lambda_r = 1 \quad (J = 1). \tag{2}$$

Where J is volume ratio and λ_i ($i = t, r, z$) are principal stretch ratios in the circumferential, axial and radial direction, respectively. The deformation mapping stretch ratios in the thick–walled tube with residual strains have the form

$$\lambda_t = \frac{\pi}{\pi - \alpha}\frac{r}{R}, \qquad \lambda_z = \frac{l}{L}, \qquad \lambda_r = \frac{\partial r}{\partial R}, \tag{3}$$

where α is the opening angle, r and l are radius and length in spatial configuration and R and L are the same in the reference configuration. Spatial configuration is defined by all mechanical loads (residual strains, axial pre–stretch, inflation by blood pressure). Spatial radius is related to undeformed one by:

$$r(R) = \sqrt{r_o^2 - \left(R_o^2 - R^2\right)\frac{\pi - \alpha}{\lambda_z \pi}}, \tag{4}$$

where r_o^2 is outer radius in the reference (undeformed) configuration. A Green strain tensor is adopted as deformation measure in the form bellow:

$$E_i = \frac{1}{2}\left(\lambda_i^2 - 1\right), \quad i = t, z, r. \tag{5}$$

There is no shear deformation in the thick–walled tube model and λ_i ($i = t, z, r$) are principal stretch ratios. Cauchy–Green strain tensor **C**, which was mentioned above, is defined in its counterparts and related to Green strain tensor by:

$$C_{ij} = \frac{\partial x_k}{\partial X_i}\frac{\partial x_k}{\partial X_j}, \quad i, j, k = t, z, r, \qquad \mathbf{C} = 2\mathbf{E} + \mathbf{I}. \tag{6,7}$$

Here **I** is identity second-order tensor. The local stress–strain relationships are given by derivatives of strain energy density function **Ψ** as:

$$\sigma_i = -p + \lambda_i^2 \frac{\partial \boldsymbol{\Psi}}{\partial E_i}, \quad i = t,r,z\,. \tag{8}$$

σ_i ($i = t,z,r$) is Cauchy (true) stress. If we consider force equilibrium in the radial direction we will obtain an equation:

$$\frac{d\sigma_r}{dr} + \frac{\sigma_r - \sigma_t}{r} = 0 \qquad \text{with boundary condition} \qquad \sigma_r(r = r_i) = -p\,. \tag{9}$$

This condition is used to determine Lagrangian multiplier p. The inner radius of the artery is denoted r_i. Using incompressibility we can transform differential equation to the form:

$$\sigma_r(r = r_i) = -p = \int_{r_i}^{r_o} \lambda_t^2 \frac{\partial \boldsymbol{\Psi}}{\partial E_t} \frac{dr}{r}\,. \tag{10}$$

Displacement related to the load pressure p can be obtained as a numerical solution of this integral. Components of the Cauchy stress tensor may be expressed using equation (8) and:

$$\sigma_r(r) = \int_{r}^{r_0} \lambda_t^2 \frac{\partial \boldsymbol{\Psi}}{\partial E_t} \frac{dr}{r}\,. \tag{11}$$

The strain energy density function is adopted in the form published by Holzapfel and Weizsäcker (1998):

$$\boldsymbol{\Psi} = c_1(I_1 - 3) + c_2\left(e^{b_1 E_t^2 + b_2 E_z^2 + b_4 E_t E_z} - 1\right) \tag{12}$$

$$E_i = \frac{1}{2}\left(\lambda_i^2 - 1\right), \; i = t, z \qquad\qquad I_1 = \lambda_t^2 + \lambda_z^2 + \lambda_r^2 \tag{13}$$

Ψ is constructed as the coupled expression, $\boldsymbol{\Psi} = \boldsymbol{\Psi}_{\text{iso}} + \boldsymbol{\Psi}_{\text{aniso}}$, isotropic part and anisotropic one. The isotropic part is related to an elastin component of the deformation of the arterial wall with material parameter c_1. That is the function of the first invariant of the Cauchy–Green strain tensor. The anisotropic part is related to the collagen bundles deformation but their deformation is not specified by any structural description, components of Cauchy–Green strain tensor related to continuous description of whole arterial wall are used. The restriction to the two–dimensional formulation is used with four material parameters c_2, b_1, b_2, b_4. The exponential shape is used with regard to large strain stiffening. For more information about the two–dimensional formulation of three–dimensional problem see Holzapfel (2000). It is worth to notice that two–dimensional restriction is also used in Holzapfe (1998) but proposed type of the strain energy density function could be extended into three dimensions, see Holzapfel (1998). Generally we can say that the first material model consider structural infomation about an arterial wall but does not take it into account in mathematical expressions.

Second model was also proposed by Holzapfel and co–workers (in Holzapfel [2000]). This model is more structurally based since authors consider arterial wall as a heterogenous fiber–reinforced continuum. We will mention only the most important facts, further information are available in the original author's paper. The structural information is incorporated into the second model by using two (reference) direction vectors $\boldsymbol{a}_{0i}$ ($i=1, 2$; $|\boldsymbol{a}_{0i}| = 1$) which characterize two families of collagen fibers in arterial walls.

$$\boldsymbol{\Psi}(\mathbf{C},\boldsymbol{a}_{01},\boldsymbol{a}_{02}) = \boldsymbol{\Psi}_{iso}(\mathbf{C}) + \boldsymbol{\Psi}_{aniso}(\mathbf{C},\boldsymbol{a}_{01},\boldsymbol{a}_{02}) \tag{14}$$

They introduced two other tensors $\mathbf{A}_1$ and $\mathbf{A}_2$ as products of $\boldsymbol{a}_{0i} \otimes \boldsymbol{a}_{0i} = \mathbf{A}_i$ ($i=1, 2$). Now they consider integrity basis for second–order tensors $\mathbf{C}$, $\mathbf{A}_1$ and $\mathbf{A}_2$ what consists of nine invariants; more details you can see in Holzapfel (2000). From these invariants they choose two denoted as $\bar{I}_4, \bar{I}_6$:

$$\bar{I}_4(\mathbf{C},\boldsymbol{a}_{01}) = \mathbf{C} : \mathbf{A}_1 \qquad \bar{I}_6(\mathbf{C},\boldsymbol{a}_{02}) = \mathbf{C} : \mathbf{A}_2 . \tag{15}$$

The final shape of $\boldsymbol{\Psi}$ is:

$$\boldsymbol{\Psi}(\mathbf{C},\boldsymbol{a}_{01},\boldsymbol{a}_{02}) = \boldsymbol{\Psi}_{iso}(\bar{I}_1) + \boldsymbol{\Psi}_{aniso}(\bar{I}_4,\bar{I}_6) = \frac{c}{2}(\bar{I}_1 - 3) + \frac{k_1}{2k_2}\sum_{j=4,6}\left(e^{k_2(\bar{I}_j - 1)^2} - 1\right). \tag{16}$$

There is a simple reason to use invariants $\bar{I}_4, \bar{I}_6$ in the constitutive theory since they are the squares of the stretches in the directions $\boldsymbol{a}_{0i}$ ($i=1, 2$), so they are stretch measures for two families of collagen fibers and therefore they have a clear physical interpretation. With the assumption that two families of the collagen fibers are presented at the same radius through whole length of a cylinder we can characterize them by vectors:

$$\boldsymbol{a}_{01} = (0, \cos\beta, \sin\beta)^T , \qquad \boldsymbol{a}_{02} = (0, \cos\beta, -\sin\beta)^T , \tag{17}$$

a cylindrical polar coordinate system is used. β is an angle between the direction of the two collagen fibers symmetrical spirals and the circumferential direction (hence a value of the spiral angle β is the same for both of the bundles of collagen fibers). If we consider this symmetry we can write structural invariants $\bar{I}_4, \bar{I}_6$ as the measures of the fiber stretches in the form:

$$\bar{I}_4 = \bar{I}_6 = \lambda^2 = \lambda_t^2 \cos^2\beta + \lambda_z^2 \sin^2\beta . \tag{18}$$

Thus strain energy density function defined in (16) could be rewrite in the form:

$$\boldsymbol{\Psi} = \frac{c}{2}(\bar{I}_1 - 3) + \frac{k_1}{k_2}\left(e^{k_2\left(\lambda_t^2 \cos^2\beta + \lambda_z^2 \sin^2\beta - 1\right)^2} - 1\right). \tag{19}$$

It is important to note that the model presented in Holzapfel (2000) is two–layered and for each arterial layer (intima + media, adventitia) is included its own SEDF, $\boldsymbol{\Psi}$. Hence the model contains 6 material parameters, 3 for each layer, and geometrical parameters as are layers thicknesses and collagen bundles angles.

3. Results

The first material model is given by the equation (12) and second one by (19). Geometrical data of the problem were obtained form artery which segments underwent residual strain measurement in 2002 in our lab. Solving of the problem was done by standard math procedures in Maple, release 8, Maple Waterloo Inc. Material parameters used in this study are adopted form literature published by authors of material models (see Holzapfel [1998, 2000]). Values of the parameters are listed below.

$$\Psi_{1998}: c_1 = 30.523 \text{ kPa}, c_2 = 0.4308 \text{ kPa}, b_1 = 5.36603 \text{ [1]}, b_2 = 3.55858 \text{ [1]}, b_4 = -31.7206;$$
$$\Psi_{2000}: c_1 = 44.24 \text{ kPa}, k_1 = 0.206 \text{ kPa}, k_2 = 1.465 \text{ [1]}. \quad (20)$$

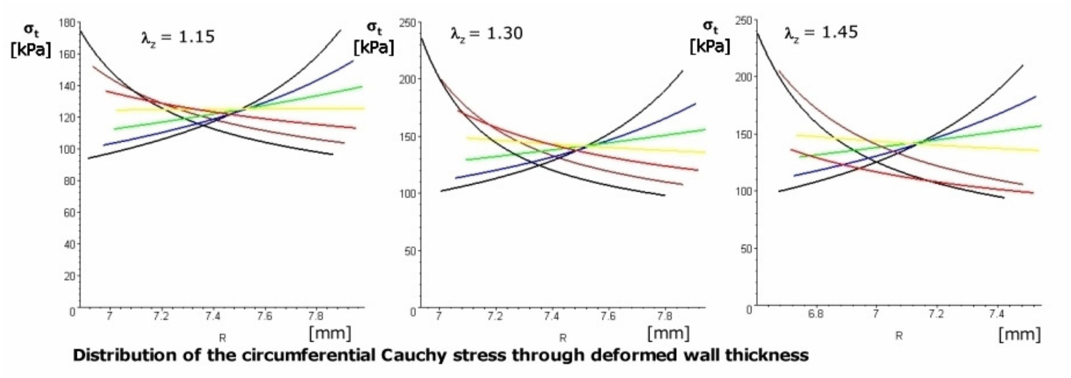

Figure 1 Ψ_{1998} Circumferential Cauchy stress

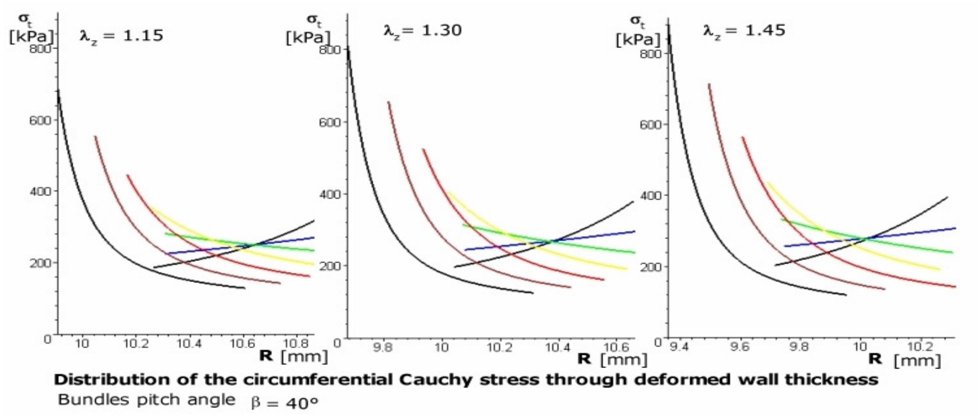

Figure 2 Ψ_{2000} Circumferential Cauchy stress

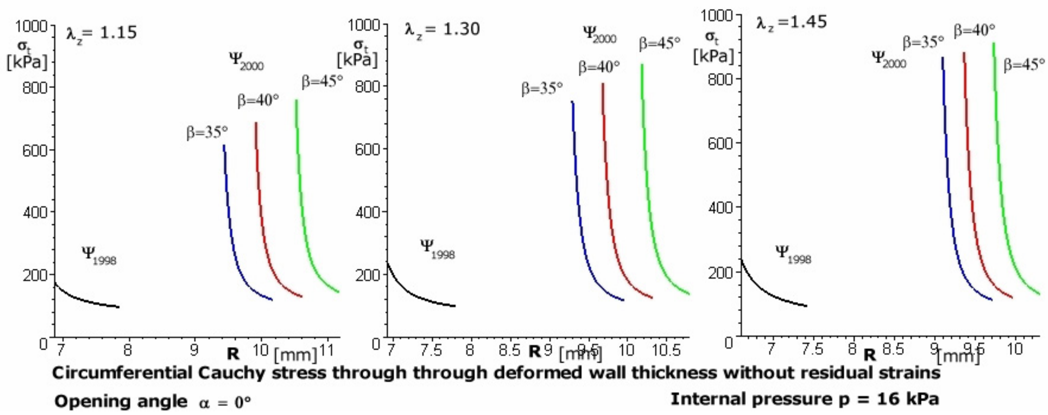

Figure 3 Influence of helical pitch angle and axial pre-stretch on Circumferential Cauchy stress

4. Conclusions

The internal load pressure corresponds to 120 mmHg. The value of axial pre–stretch is one of the most important inputs to the model. The used axial pre-stretch values (15, 30 and 45%) correspond to possible physiological values but real in-situ values of the axial pre-stretch still remain as a question since a literature is not unique in this. Possible values range from λ_z = 1.05 to approximately λ_z = 1.45.

So, in this paper two material models were compared in the case of physiological loading. The first model showed typical behavior of thick–walled tube. Determined displacements and computed stress fields range close to expected values. The circumferential stress between 200 – 250 kPa is commonly considered as a stress state similar to smooth muscle cells in vivo states. Second model, what is utilized for two–layered computational model, showed significant influence of residual strains on a shape of stress–radius curves and on the stress values also. It seems to be necessary to suppose high values of an opening angle. Residual strains have to exceed opening angle of 90° to manage stress field close to supposed physiological range.

The shape of the stress curves did not change significantly by varying the pitch angle close to β = 40° value but the curves are shifted and the increase of the longitudinal pre–stretch causes convergence of circumferential stress curves. Second model is also significantly more compliant than first one and un–physiological values of predicted inner radius were achieved within the model. But it is important to note that second layer was not considered in this model.

5. References

Holzapfel, G.A. and Weizsäcker, H.W. 1998 Biomechanical behavior of the arterial wall and its numerical characterization. *Comp. Biol. Med.* **28** 377–392.

Holzapfel, G. A., Gasser, T. C. and Ogden, R. W. 2000 A new constitutive framework for arterial wall mechanics and a comparative study of material models. *J. Elast.* **61** 1–48.

Holzapfel, G.A., Gasser, T.C., and Ogden, RW. 2004 Comparison of a multi-layer structural model forarterial walls with a Fung-type model, and issues of material stability. *J Biomech Eng* **126** 264–275.

Holzapfel, G.A, Sommer, G., Gasser, C.T. and Regitnig, P. 2005 Determination of layer-specific mechanical properties of human coronary arteries with nonatherosclerotic intimal thickening and related constitutive modeling. *Am. J. Physiol. Heart. Circ. Physiol.* **289** 2048–2058

Matsumoto, T. and Hayashi, K. 1996 Stress and strain distribution in hypertensive and normotensive rat aorta considering residual strain. *J. Biomech. Eng*. **118** 62–72.

6. Acknowledgement

This research has been supported by MSM 68 40 77 00 12 and GA CR 106/04/1181.